

# Physics with Atmospheric Tau Neutrino at ICAL-INO

Sanjib Kumar Agarwalla

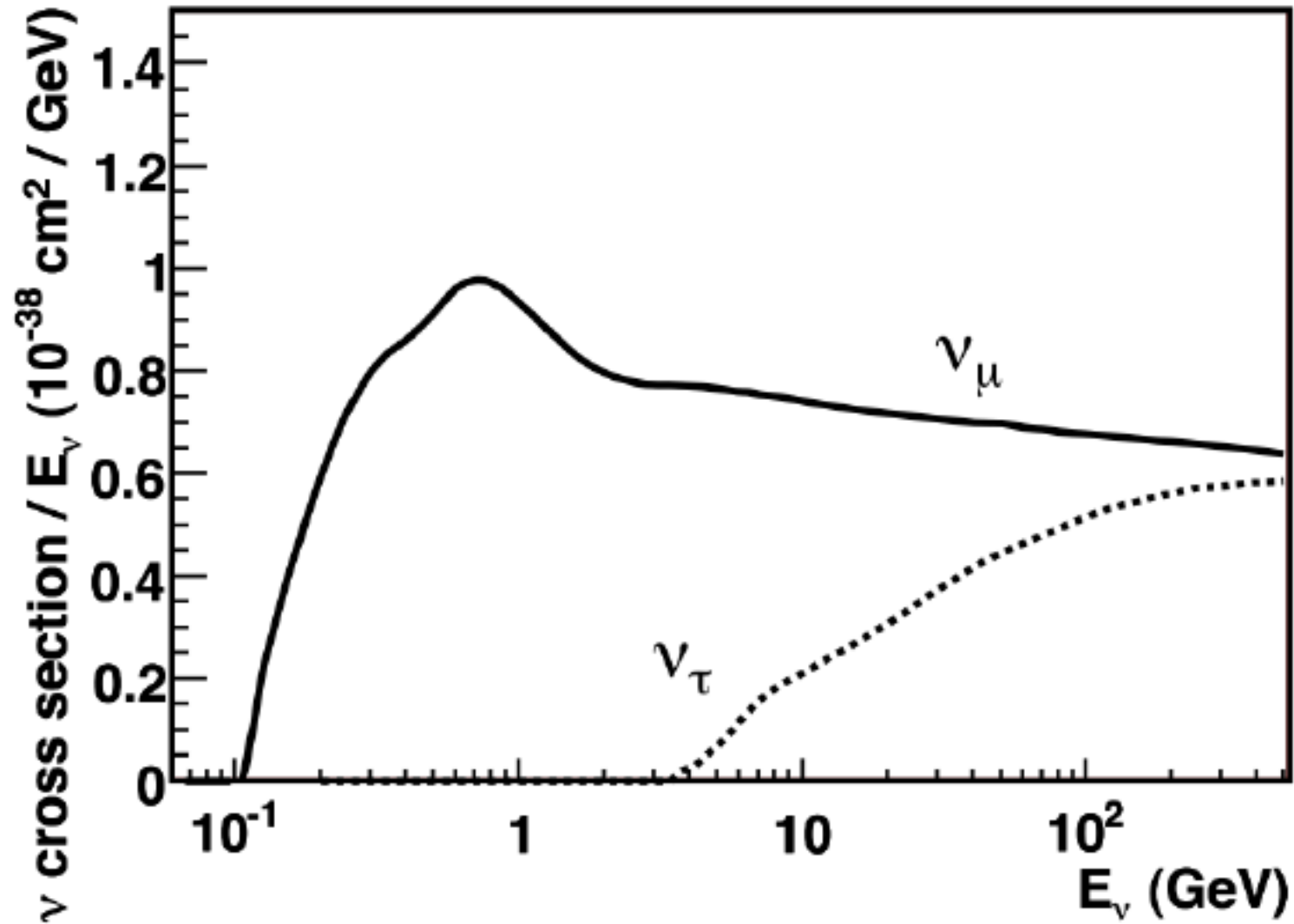
Institute of Physics (IOP), Bhubaneswar, Odisha, India

[sanjib@iopb.res.in](mailto:sanjib@iopb.res.in)

<https://twitter.com/sanjibneutrino>



# $\nu_\mu$ and $\nu_\tau$ cross sections



Formaggio, Zeller, arXiv:1305.7513 [hep-ex]

# $\tau$ lepton decay modes

Leptonic decay modes:

$$\left. \begin{aligned} \tau &\Rightarrow \nu_\tau + \nu_e + e \quad (17.4\%) \\ \tau &\Rightarrow \nu_\tau + \nu_\mu + \mu \quad (17.8\%) \end{aligned} \right\} \sim 35\%$$

Hadronic decay modes:

$$\left. \begin{aligned} &\text{1 prong} \\ \tau &\Rightarrow \nu_\tau + \pi^\pm \quad (11\%) \\ \tau &\Rightarrow \nu_\tau + \pi^\pm + \pi^0 \quad (25.4\%) \\ \tau &\Rightarrow \nu_\tau + \pi^\pm + \pi^0 + \pi^0 \quad (10.8\%) \\ \tau &\Rightarrow \nu_\tau + \pi^\pm + \pi^0 + \pi^0 + \pi^0 \quad (1.4\%) \\ \tau &\Rightarrow \nu_\tau + \pi^\pm + K^\pm + n \pi^0 \quad (1.6\%) \\ &\text{3 prong} \\ \tau &\Rightarrow \nu_\tau + 3 \pi^\pm + n \pi^0 \quad (15.2\%) \end{aligned} \right\} \sim 65\%$$

$\sim 77\%$  (for the 1 prong group)

$\sim 23\%$  (for the 3 prong group)

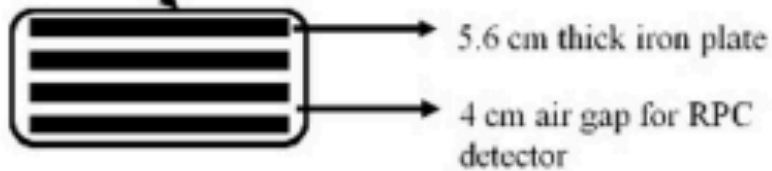
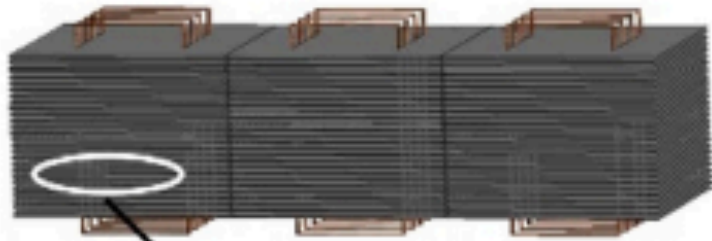
How to detect them?

Hadronic showers deposit energy inside the Iron Calorimeter

We calibrate this energy by counting the no. of hits due to these hadrons

from PDG

# Iron Calorimeter (ICAL) Detector at INO [Design and Specifications]



ICAL	
No. of modules	3
Module dimension	16 m × 16 m × 14.5 m
Detector dimension	48 m × 16 m × 14.5 m
No. of layers	151
Iron plate thickness	5.6 cm
Gap for RPC trays	4.0 cm
Magnetic field	1.5 Tesla
RPC	
RPC unit dimension	2 m × 2 m
Readout strip width	3 cm
No. of RPC units/Layer/Module	64
Total no. of RPC units	~ 30,000
No. of electronic readout channels	$3.9 \times 10^6$

Resistive Plate Chambers (RPCs) act as active element

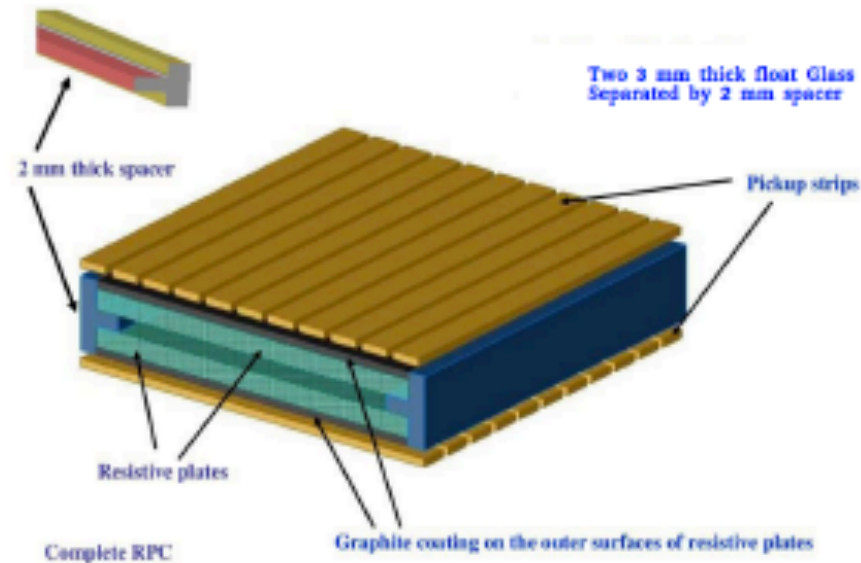
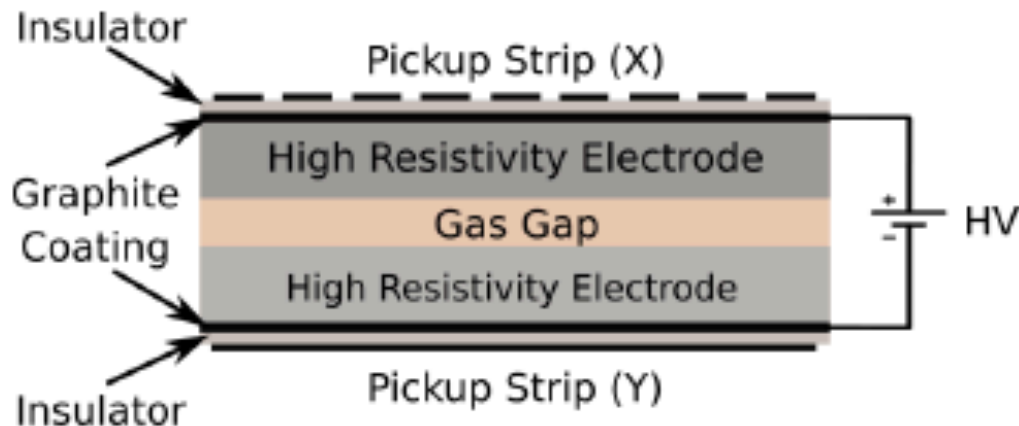
5.6 cm thick iron plates act as target material

Present design of ICAL not suitable to detect electrons

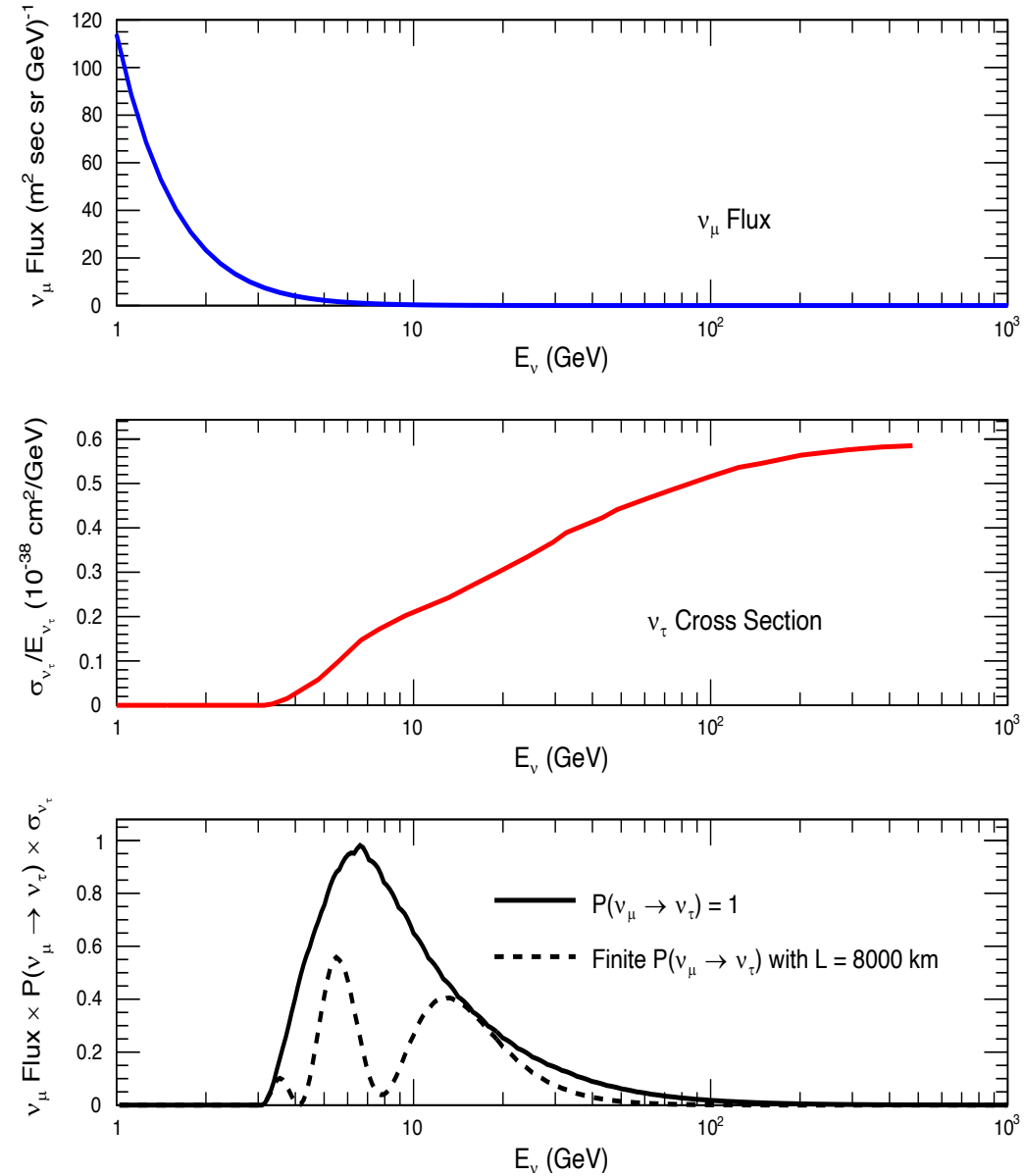
ICAL can measure muon energy and direction quite precisely

It can measure hadron energy and can distinguish between up-going and down-going hadrons

50 kt magnetized ( $> 1$  Tesla) ICAL detector – charge identification capability (CID) helps to distinguish  $\mu^-$  and  $\mu^+$  events



# Basics of $\nu_\tau$ Detection at ICAL@INO



Courtesy Anil Kumar

# Detecting $\nu_\tau$ at ICAL@INO using Hadron Showers

Atmospheric neutrinos are of  $\nu_\mu$  and  $\nu_e$  flavours, but we get  $\nu_\tau$  through mass-induced flavour oscillation, mostly in the upward direction because of long path lengths (also close to maximal value of  $\theta_{23}$  helps)

Charged Current (CC) interactions of  $\nu_\tau$  with ICAL (Fe) suppressed due to large tau mass (threshold energy for this interaction is  $\sim 3.5$  GeV) and flux of atmospheric neutrinos falls rapidly with energy

Such tau leptons decay through hadronic channel with a branching ratio of  $\sim 65\%$ . Hence, we have two sources of hadrons in CC tau events:

$$\begin{aligned} \nu_\tau + N &\Rightarrow \tau + X \text{ (hadrons)} \\ &\quad \downarrow \sum_i h_i + \nu_\tau \end{aligned}$$

Neutral Current (NC) events also produce hadrons in the detector

$$\nu_\alpha + N \Rightarrow \nu_\alpha + X$$

Therefore, tau events occur with same signature as NC events in ICAL

# Detecting $\nu_\tau$ at ICAL@INO using Hadron Showers

NUANCE neutrino event generator (version 3.5) used to generate the events using Honda – 3D atmospheric neutrino fluxes

Full three-flavour neutrino oscillation probabilities applied using the PREM profile of the Earth

The reconstruction efficiency of hadrons is a function of their energy and direction [taken from M. M. Devi et al., JINST 13 (2018) 03], improves with energy and  $|\cos\theta|$

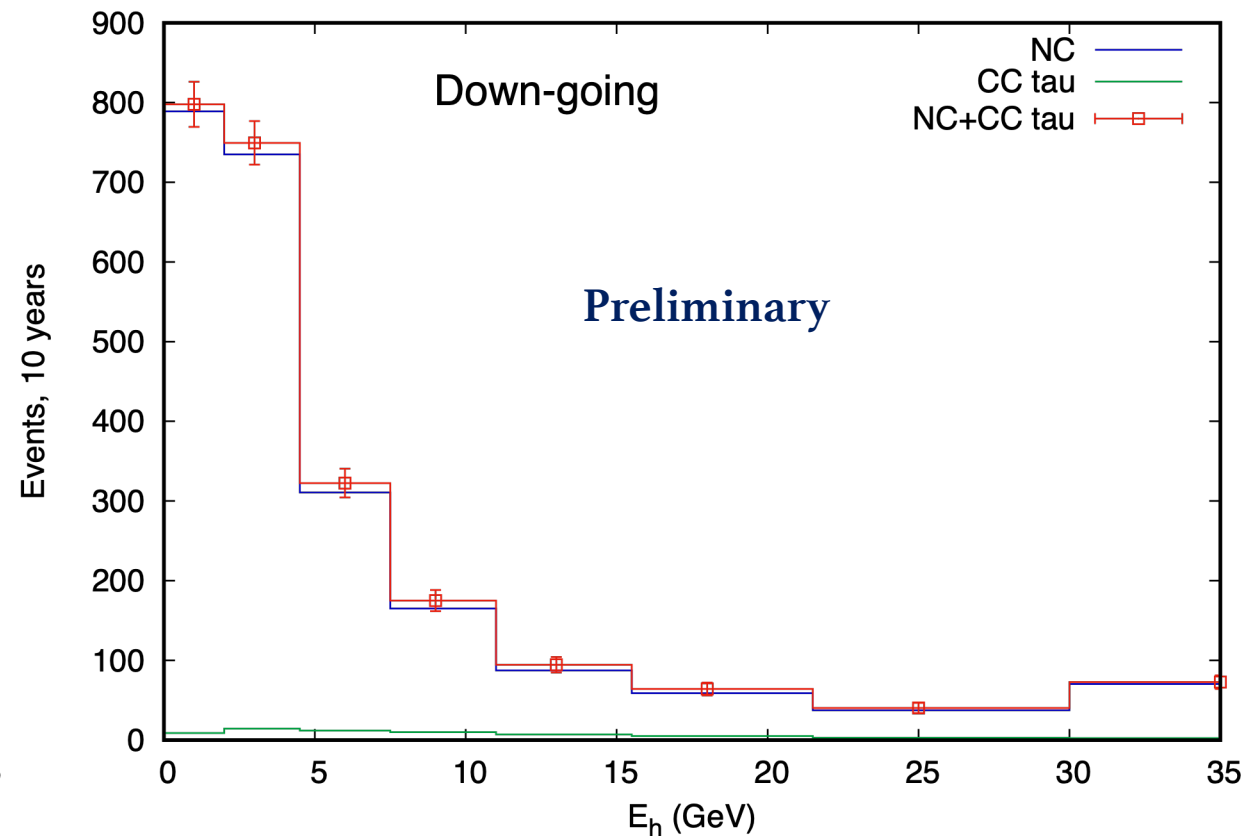
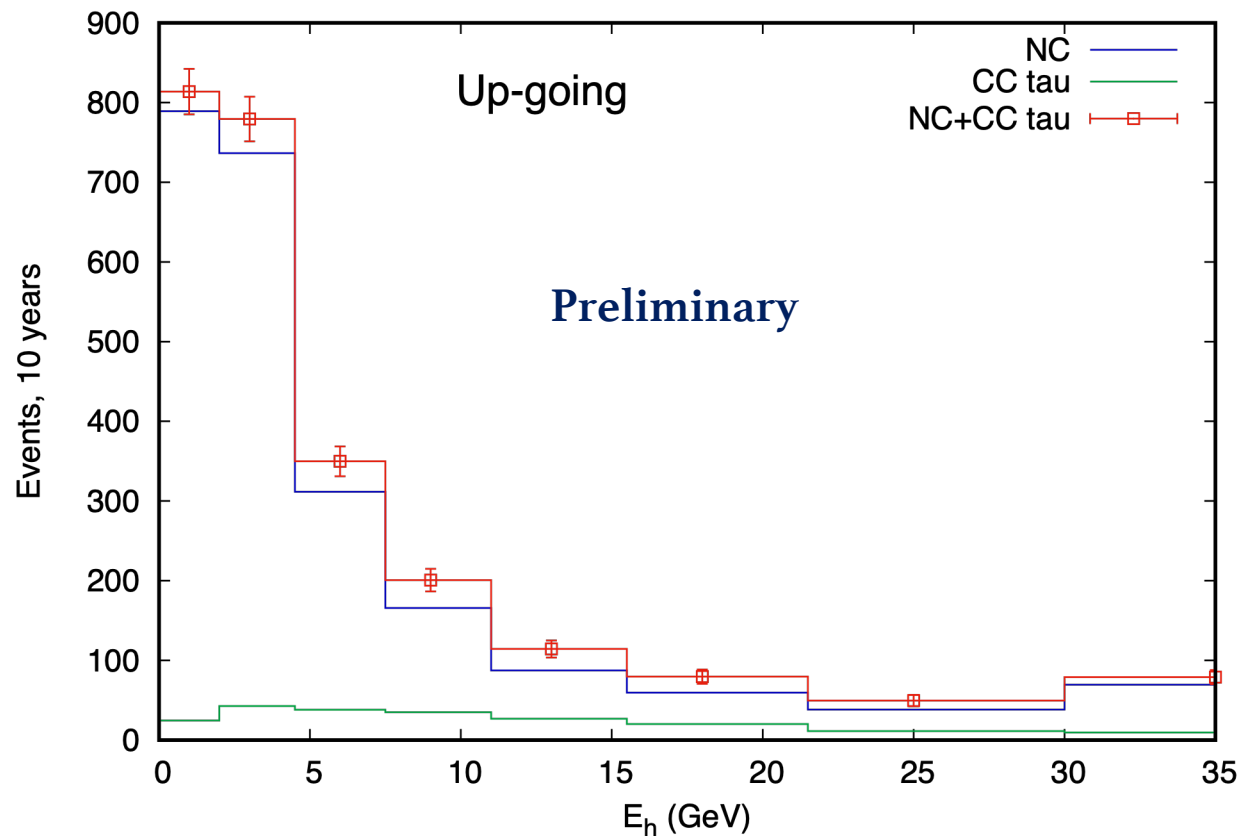
Hadron reconstruction efficiency is  $> 90\%$  for energies above 2 GeV or so

The direction reconstruction efficiency of hadrons is defined as the fraction of events that gets reconstructed in the “correct” half-plane. That is, an up event is reconstructed as up and down as down

Around 80% directional reconstruction efficiency for vertical events and no directional sensitivity for near-horizon events

Hadron energy resolution is taken from (M .M. Devi et al., 2013 JINST 8 P11003), which is about 40% to 60% in the energy range of 2 to 8 GeV and about 40% for energies above 8 GeV

# Detecting $\nu_\tau$ at ICAL@INO using Hadron Showers



R. Thirusenthil, D. Indumathi, in progress (on behalf of the INO Collaboration)

Two bins for hadron directions (up-going and down-going). We get non-zero down-going hadron events because of direction mis-id of hadrons, but we have more up-going tau events and maximum sensitivity comes from these events



# Detecting $\nu_\tau$ at ICAL@INO using Hadron Showers

Systematic errors introduced through pulls: overall flux normalization (20%), cross section uncertainties (10%), zenith angle error (5%), energy dependence of the spectra (tilt error from Honda et al., arXiv:1908.08765), and overall detector uncertainty of 5%

If tau events are ignored, so simulated “data” is fitted only to NC events, we obtain  $\Delta\chi^2 = 35.3$ , indicating the sensitivity to tau events

When systematic errors are included, the sensitivity to tau detection decreases to  $\Delta\chi^2 = 15.7$ . Flux uncertainties significantly reduced the sensitivity

When an energy cut of  $E > 3$  GeV applied to remove low-energy CC  $\mu$  events that can mimic NC events (when muon track is missed), we obtain  $\Delta\chi^2 = 14.6$

Hence, ICAL will be **sensitive to tau events to about  $3.8\sigma$**  (median sensitivity) in 10 years with 50 kt magnetized ICAL detector.

R. Thirusenthil, D. Indumathi, in progress (on behalf of the INO Collaboration)

# $\nu_\mu \rightarrow \nu_\tau$ transition with NSI parameter $\epsilon_{\mu\tau}$

Assuming that oscillations due to solar mass-squared difference is suppressed, 1-3 mixing angle is zero, and 2-3 mixing angle is 45 degree

$$P_{\nu_\mu \rightarrow \nu_\tau} = \sin^2 \left[ L_\nu \left( \frac{\Delta m_{32}^2}{4E_\nu} + \epsilon_{\mu\tau} V_{CC} \right) \right]$$

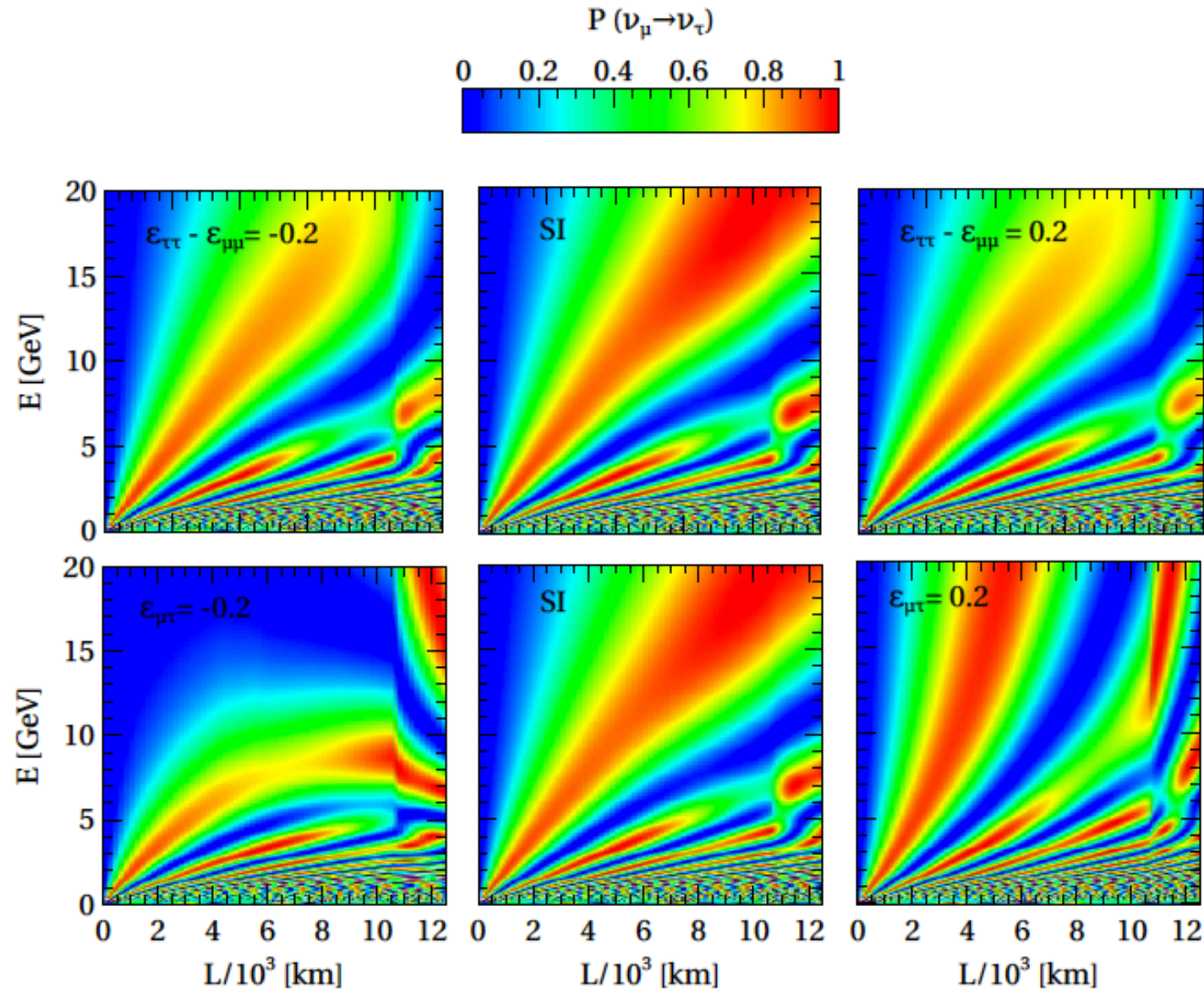
$$P_{\nu_\mu \rightarrow \nu_\tau}^m \simeq \left[ 1 - \frac{(\epsilon_{\tau\tau} - \epsilon_{\mu\mu})^2 \hat{A}^2}{(1 + 2\epsilon_{\mu\tau} \hat{A})^2} \right] \times \sin^2 \left[ \left\{ 1 + 2\epsilon_{\mu\tau} \hat{A} + \frac{1}{2} \frac{(\epsilon_{\tau\tau} - \epsilon_{\mu\mu})^2 \hat{A}^2}{(1 + 2\epsilon_{\mu\tau} \hat{A})} \right\} \frac{\Delta m_{31}^2 L}{4E} \right]$$

Gonzalez-Garcia, Maltoni, hep-ph/0404085

Mocioiu, Wright, arXiv:1410.6193 [hep-ph]

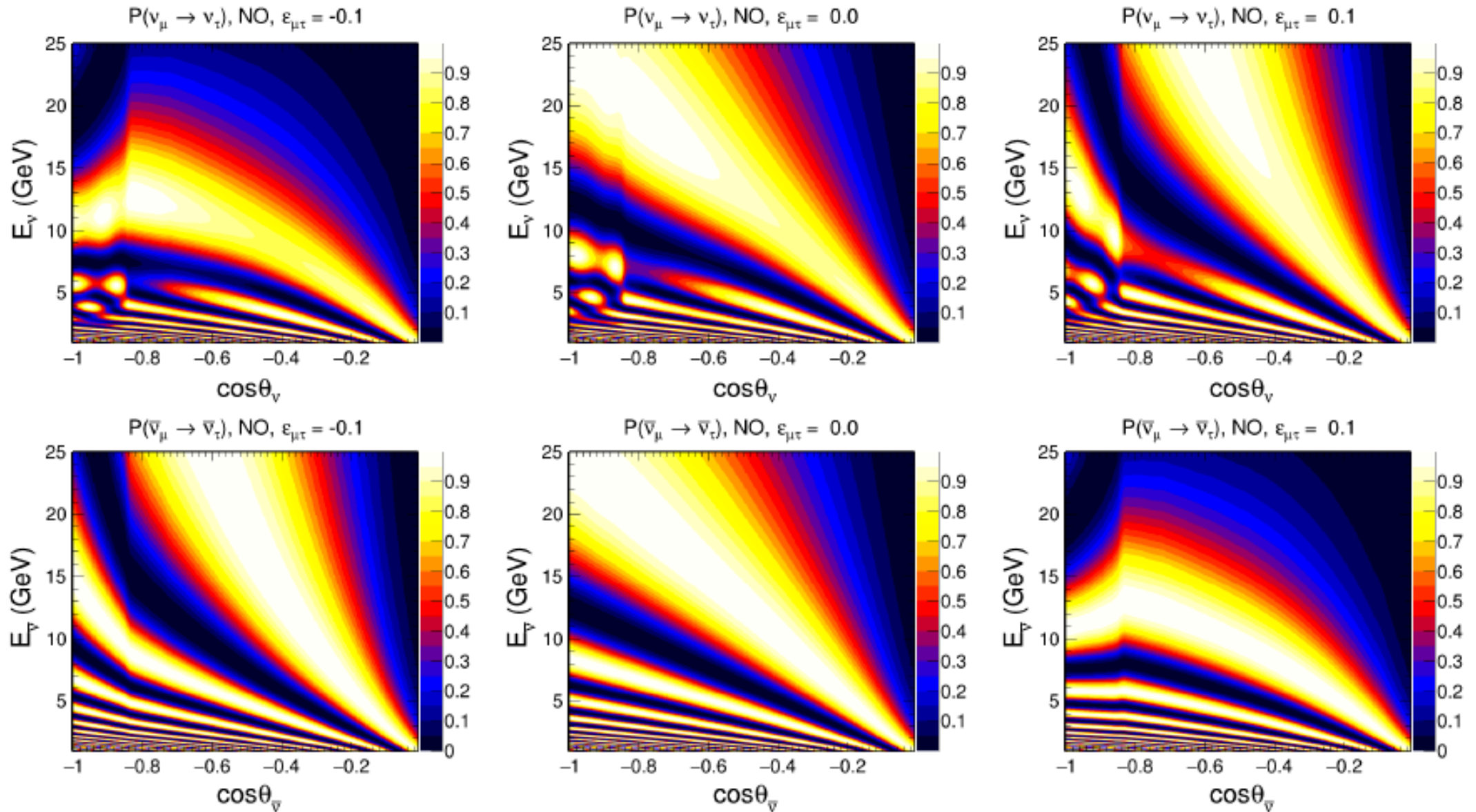
Agarwalla, Das, Masud, Swain, arXiv:2103.13431 [hep-ph]

# $\nu_\mu \rightarrow \nu_\tau$ transition with NSI parameters from 2-3 Block



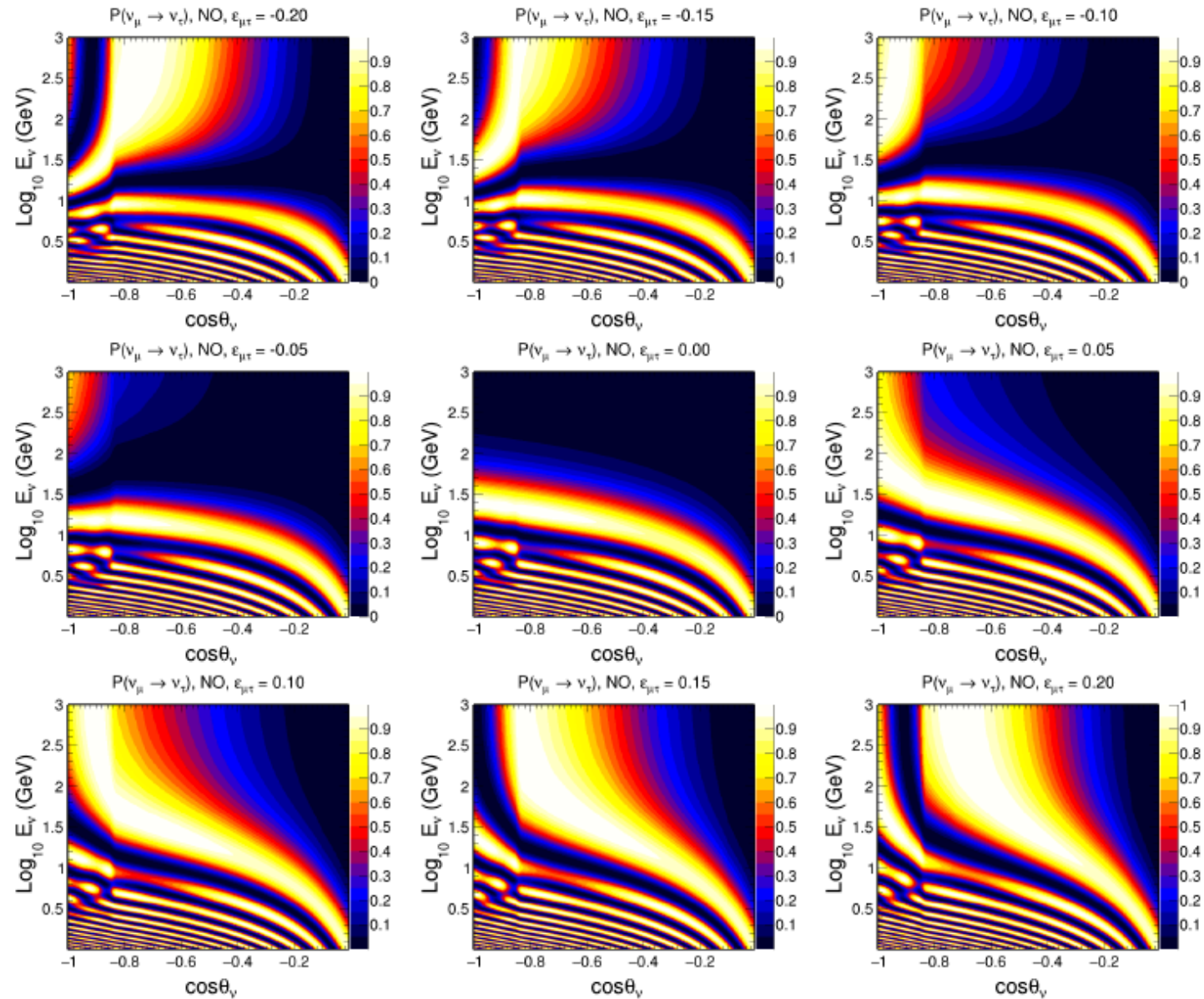
Agarwalla, Das, Masud, Swain, arXiv:2103.13431 [hep-ph]

# $\nu_\mu \rightarrow \nu_\tau$ transition with NSI parameter $\epsilon_{\mu\tau}$

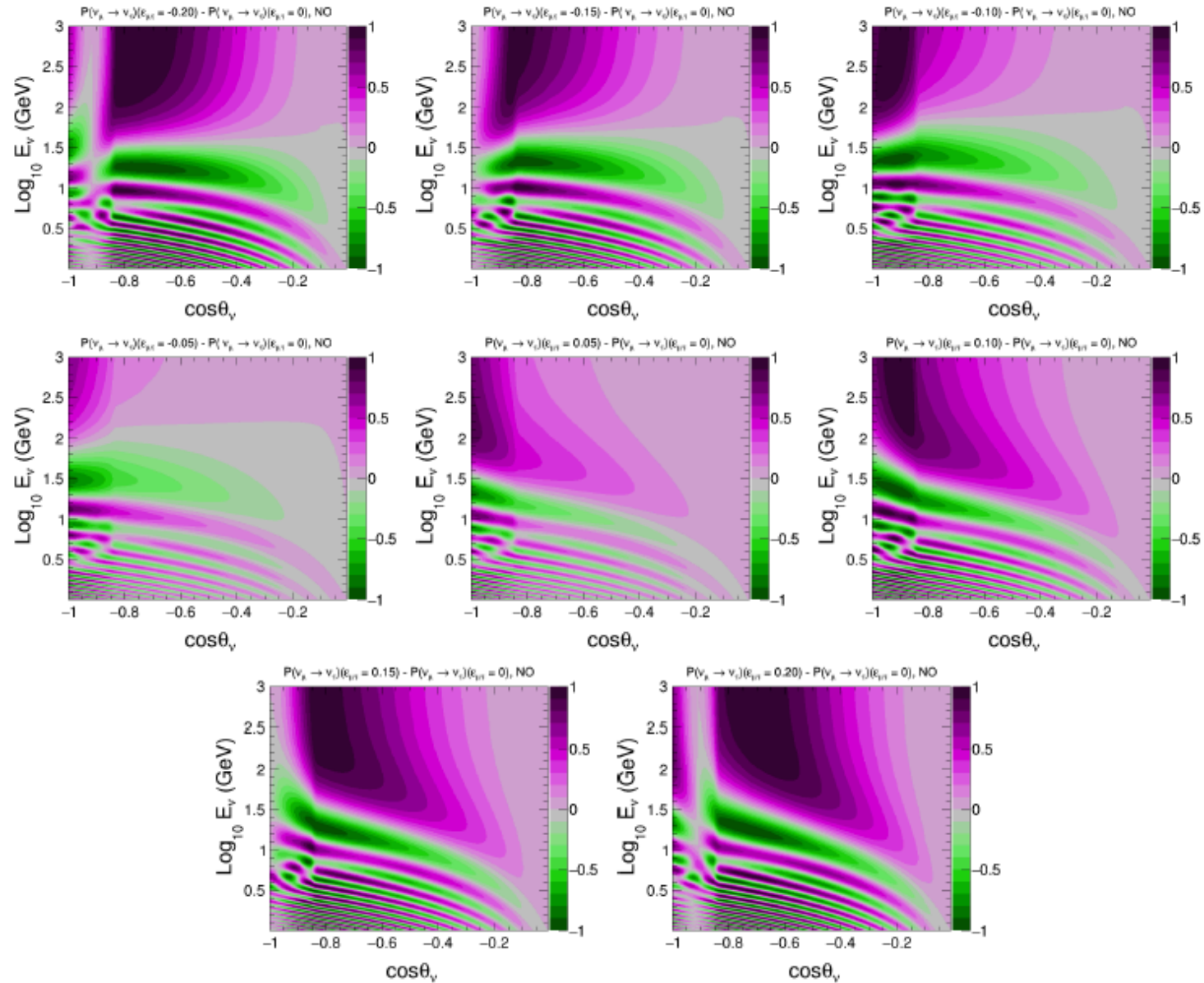




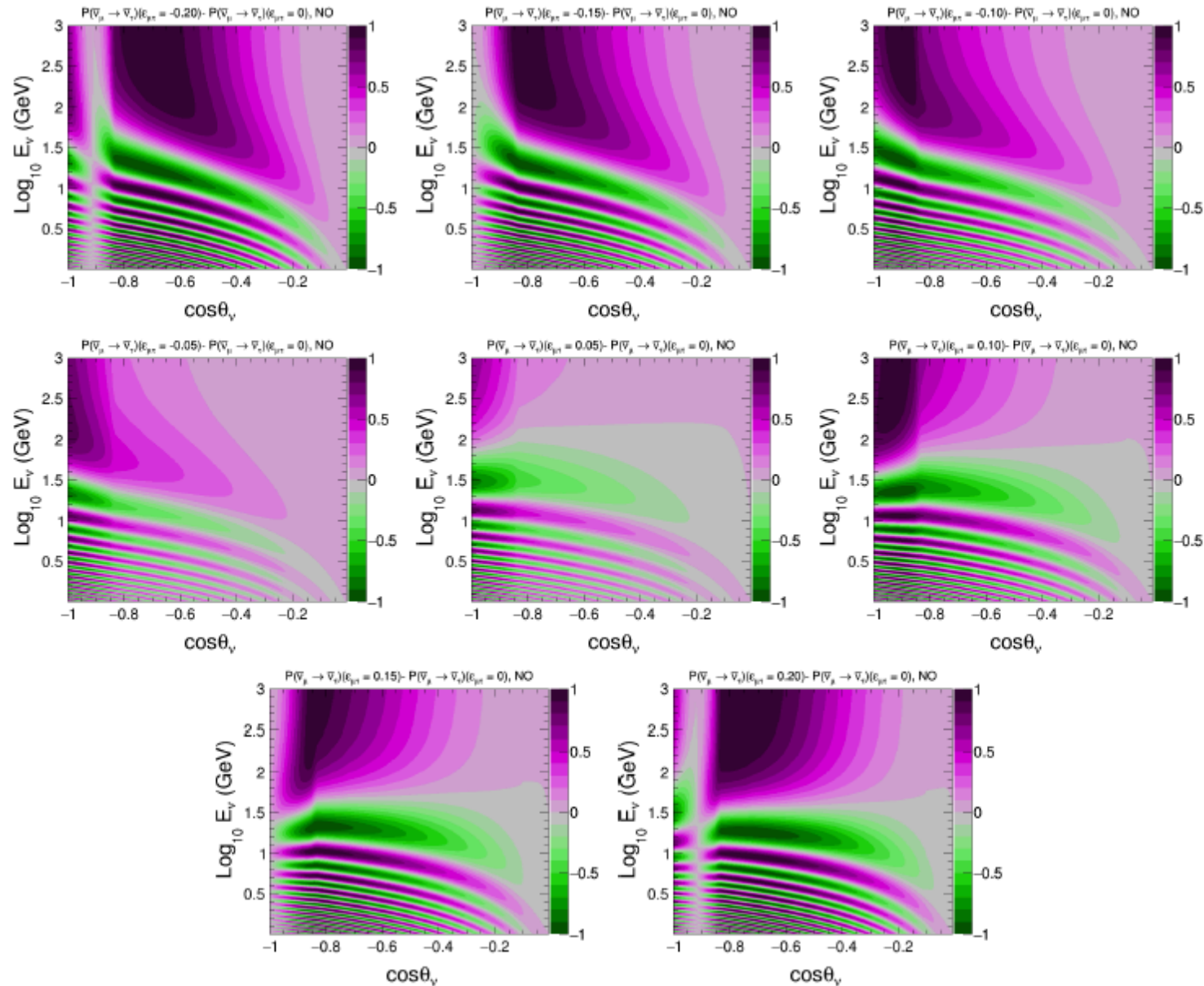
# $\nu_\mu \rightarrow \nu_\tau$ transition with NSI parameter $\epsilon_{\mu\tau}$ [1 – 1000 GeV]



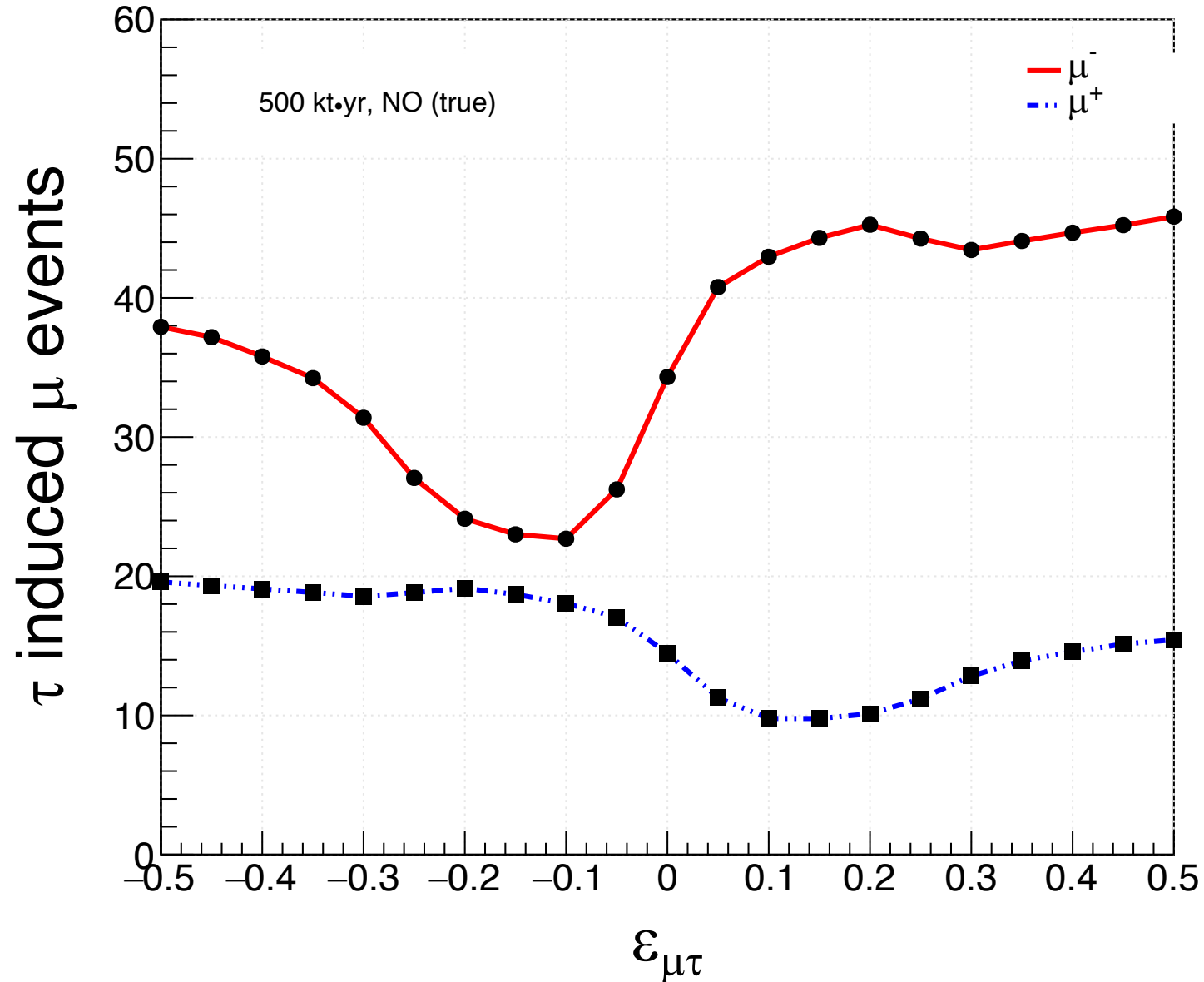
# $\nu_\mu \rightarrow \nu_\tau$ [NSI] - $\nu_\mu \rightarrow \nu_\tau$ [SI] in [1 - 1000 GeV]



# $\bar{\nu}_\mu \rightarrow \bar{\nu}_\tau$ [NSI] - $\bar{\nu}_\mu \rightarrow \bar{\nu}_\tau$ [SI] in [I - 1000 GeV]



# Muon events from Tau decay with NSI parameter $\epsilon_{\mu\tau}$

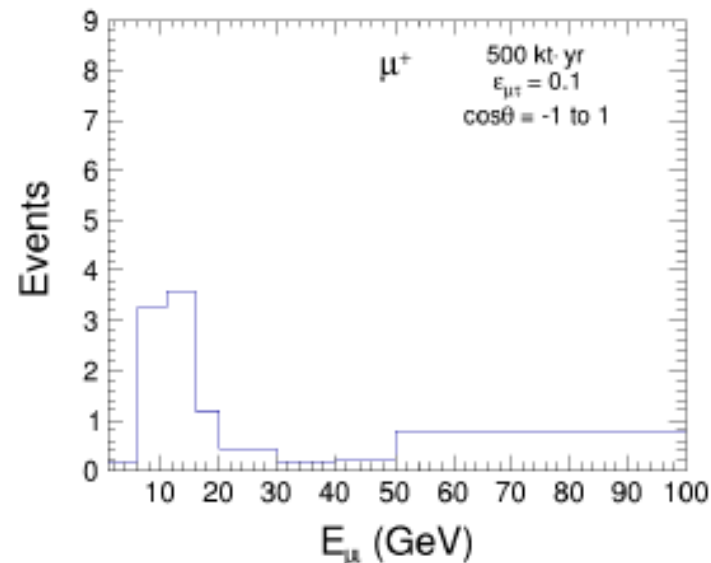
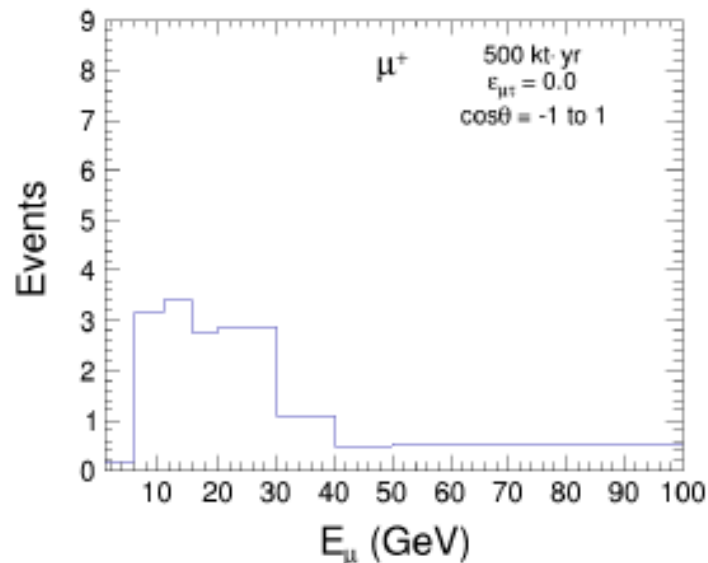
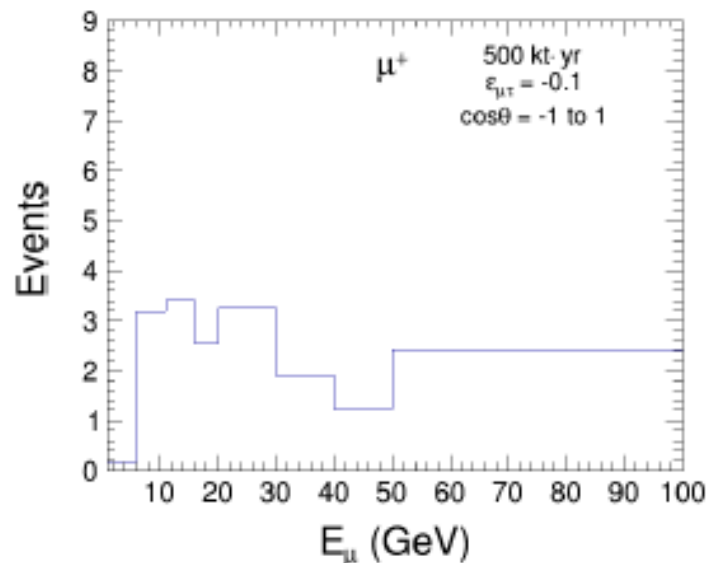
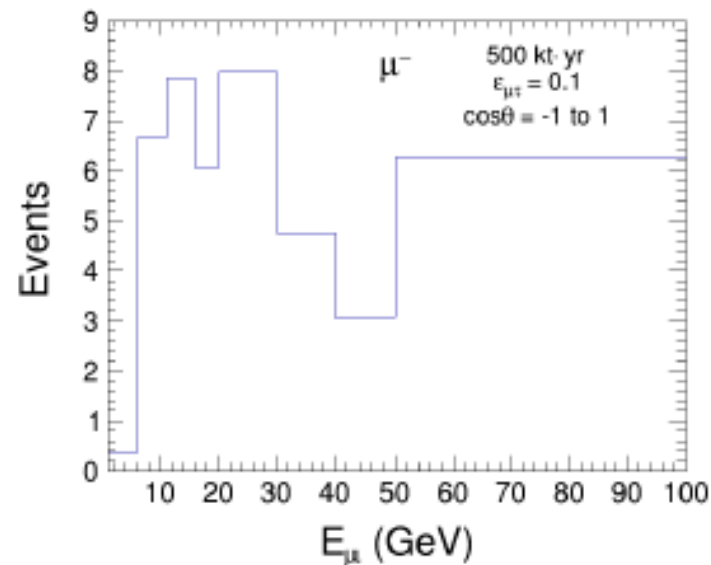
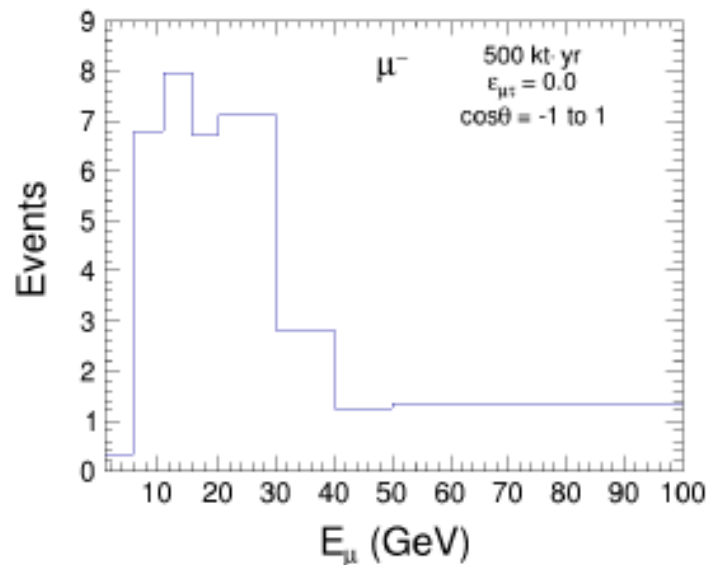
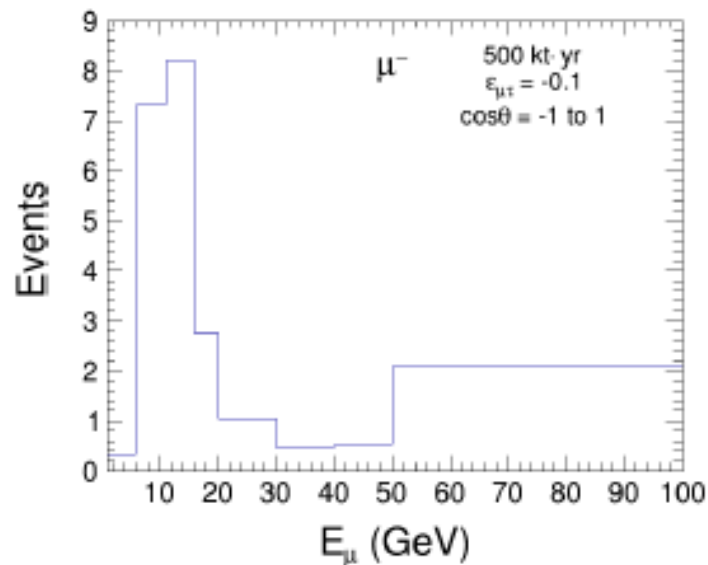


muon neutrino energy range: 1 GeV to 100 GeV  
muon neutrino zenith angle range ( $\cos\theta$ ): -1 to 1  
no detector properties are included

Kumar, Khatun, Agarwalla, in progress



# Muon events from Tau decay with NSI parameter $\epsilon_{\mu\tau}$



Kumar, Khatun, Agarwalla, in progress

# $\nu_\mu \rightarrow \nu_\tau$ transition with NSI parameters

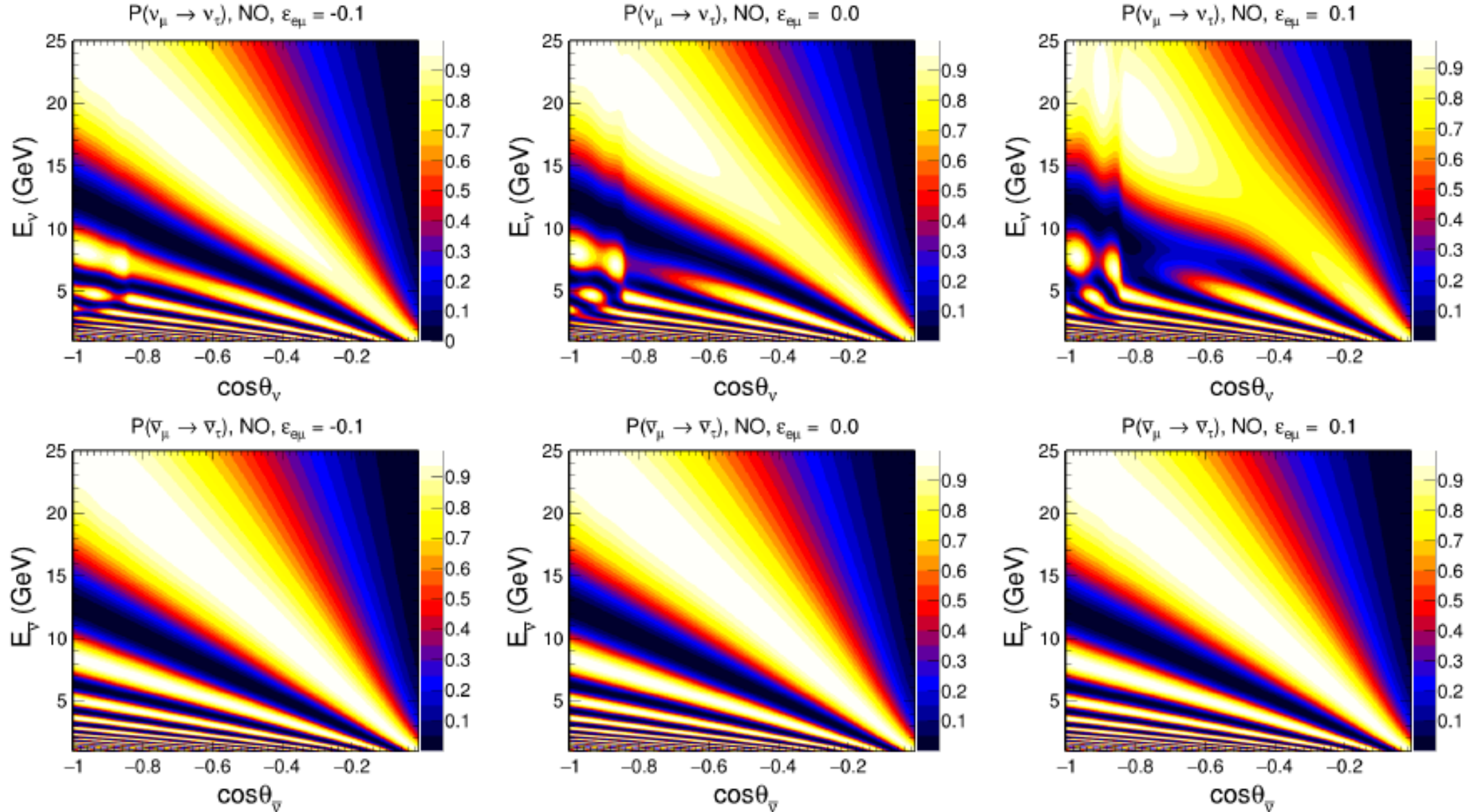
$$\begin{aligned}
 P(\nu_\mu \rightarrow \nu_\tau) &= 1 - P(\nu_\mu \rightarrow \nu_\mu) - P(\nu_\mu \rightarrow \nu_e) \\
 &= s_{2 \times 23}^2 \sin^2 \frac{\Delta m_{31}^2 L}{4E} - 4\tilde{s}_{13}^2 s_{23}^2 \sin^2 \frac{(\Delta m_{31}^2 - a_{CC})L}{4E} \\
 &\quad - \left( \frac{\Delta m_{21}^2}{\Delta m_{31}^2} \right)^2 c_{23}^2 s_{2 \times 12}^2 \left( \frac{\Delta m_{31}^2}{a_{CC}} \right)^2 \sin^2 \frac{a_{CC}L}{4E} \\
 &\quad + \frac{\Delta m_{21}^2}{\Delta m_{31}^2} \tilde{s}_{13} s_{2 \times 12} s_{2 \times 23} \frac{\Delta m_{31}^2}{a_{CC}} \left[ \sin^2 \frac{a_{CC}L}{4E} - \sin^2 \frac{\Delta m_{31}^2 L}{4E} + \sin^2 \frac{(\Delta m_{31}^2 - a_{CC})L}{4E} \right] \\
 &\quad + 4\epsilon_{e\mu}^m \tilde{s}_{13} s_{23} c_{23}^2 \left[ \sin^2 \frac{a_{CC}L}{4E} - \sin^2 \frac{\Delta m_{31}^2 L}{4E} + \sin^2 \frac{(\Delta m_{31}^2 - a_{CC})L}{4E} \right] \\
 &\quad - 8\epsilon_{e\mu}^m \tilde{s}_{13} s_{23}^3 \frac{a_{CC}}{\Delta m_{31}^2 - a_{CC}} \sin^2 \frac{(\Delta m_{31}^2 - a_{CC})L}{4E} \\
 &\quad - 4\epsilon_{e\mu}^m \frac{\Delta m_{21}^2}{\Delta m_{31}^2} s_{2 \times 12} c_{23}^3 \frac{\Delta m_{31}^2}{a_{CC}} \sin^2 \frac{a_{CC}L}{4E} \\
 &\quad + 2\epsilon_{e\mu}^m \frac{\Delta m_{21}^2}{\Delta m_{31}^2} s_{2 \times 12} s_{23}^2 c_{23} \frac{\Delta m_{31}^2}{\Delta m_{31}^2 - a_{CC}} \left[ \sin^2 \frac{a_{CC}L}{4E} - \sin^2 \frac{\Delta m_{31}^2 L}{4E} + \sin^2 \frac{(\Delta m_{31}^2 - a_{CC})L}{4E} \right] \\
 &\quad - 4\epsilon_{e\tau}^m \tilde{s}_{13} s_{23}^2 c_{23} \left[ \sin^2 \frac{a_{CC}L}{4E} - \sin^2 \frac{\Delta m_{31}^2 L}{4E} + \sin^2 \frac{(\Delta m_{31}^2 - a_{CC})L}{4E} \right] \\
 &\quad - 8\epsilon_{e\tau}^m \tilde{s}_{13} s_{23}^2 c_{23} \frac{a_{CC}}{\Delta m_{31}^2 - a_{CC}} \sin^2 \frac{(\Delta m_{31}^2 - a_{CC})L}{4E} \\
 &\quad + 4\epsilon_{e\tau}^m \frac{\Delta m_{21}^2}{\Delta m_{31}^2} s_{2 \times 12} s_{23} c_{23}^2 \frac{\Delta m_{31}^2}{a_{CC}} \sin^2 \frac{a_{CC}L}{4E} \\
 &\quad + 2\epsilon_{e\tau}^m \frac{\Delta m_{21}^2}{\Delta m_{31}^2} s_{2 \times 12} s_{23} c_{23}^2 \frac{\Delta m_{31}^2}{\Delta m_{31}^2 - a_{CC}} \left[ \sin^2 \frac{a_{CC}L}{4E} - \sin^2 \frac{\Delta m_{31}^2 L}{4E} + \sin^2 \frac{(\Delta m_{31}^2 - a_{CC})L}{4E} \right] \\
 &\quad + \mathcal{O}(s_{13}) + \mathcal{O}(s_{13}^3) + \mathcal{O}(\epsilon s_{13}^2) + \mathcal{O}(\epsilon^2) \\
 &\quad + \mathcal{O}\left(\frac{\Delta m_{21}^2}{\Delta m_{31}^2}\right) + \mathcal{O}\left(\left[\frac{\Delta m_{21}^2}{\Delta m_{31}^2}\right]^3\right) + \mathcal{O}\left(\left[\frac{\Delta m_{21}^2}{\Delta m_{31}^2}\right]^2 s_{13}\right) + \mathcal{O}\left(\frac{\Delta m_{21}^2}{\Delta m_{31}^2} s_{13}^2\right) \\
 &\quad + \mathcal{O}\left(\epsilon \left[\frac{\Delta m_{21}^2}{\Delta m_{31}^2}\right]^2\right) + \mathcal{O}\left(\epsilon s_{13} \frac{\Delta m_{21}^2}{\Delta m_{31}^2}\right).
 \end{aligned}$$

where,

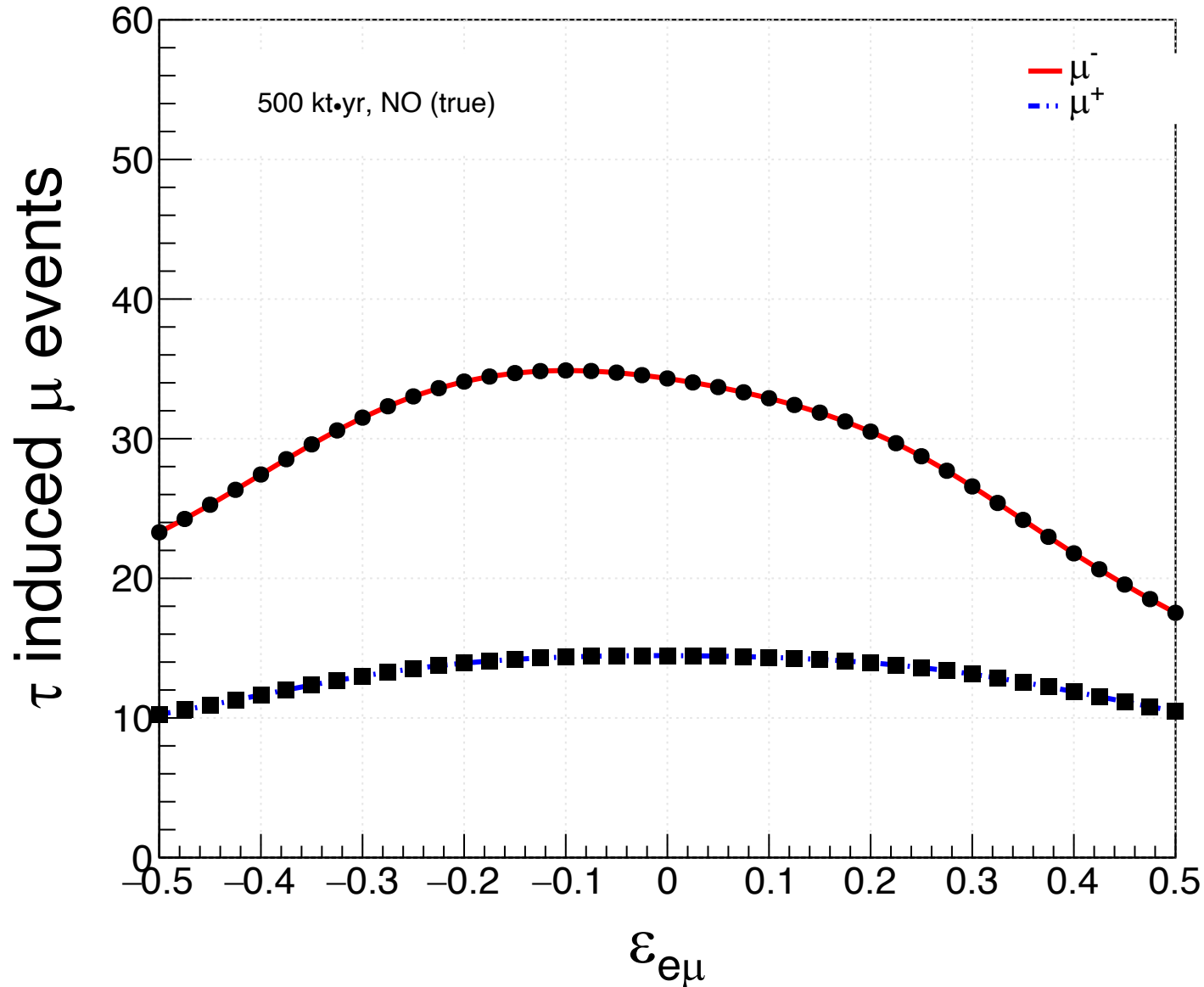
$$\tilde{s}_{13} \equiv \frac{\Delta m_{31}^2}{\Delta m_{31}^2 - a_{CC}} s_{13} + \mathcal{O}(s_{13}^2).$$

Derived from Kopp, Lindner, Ota, Sato, arXiv:0708.0152 [hep-ph]  
 Courtesy Sadashiv Sahoo

# $\nu_\mu \rightarrow \nu_\tau$ transition with NSI parameter $\epsilon_{e\mu}$



# Muon events from Tau decay with NSI parameter $\epsilon_{e\mu}$

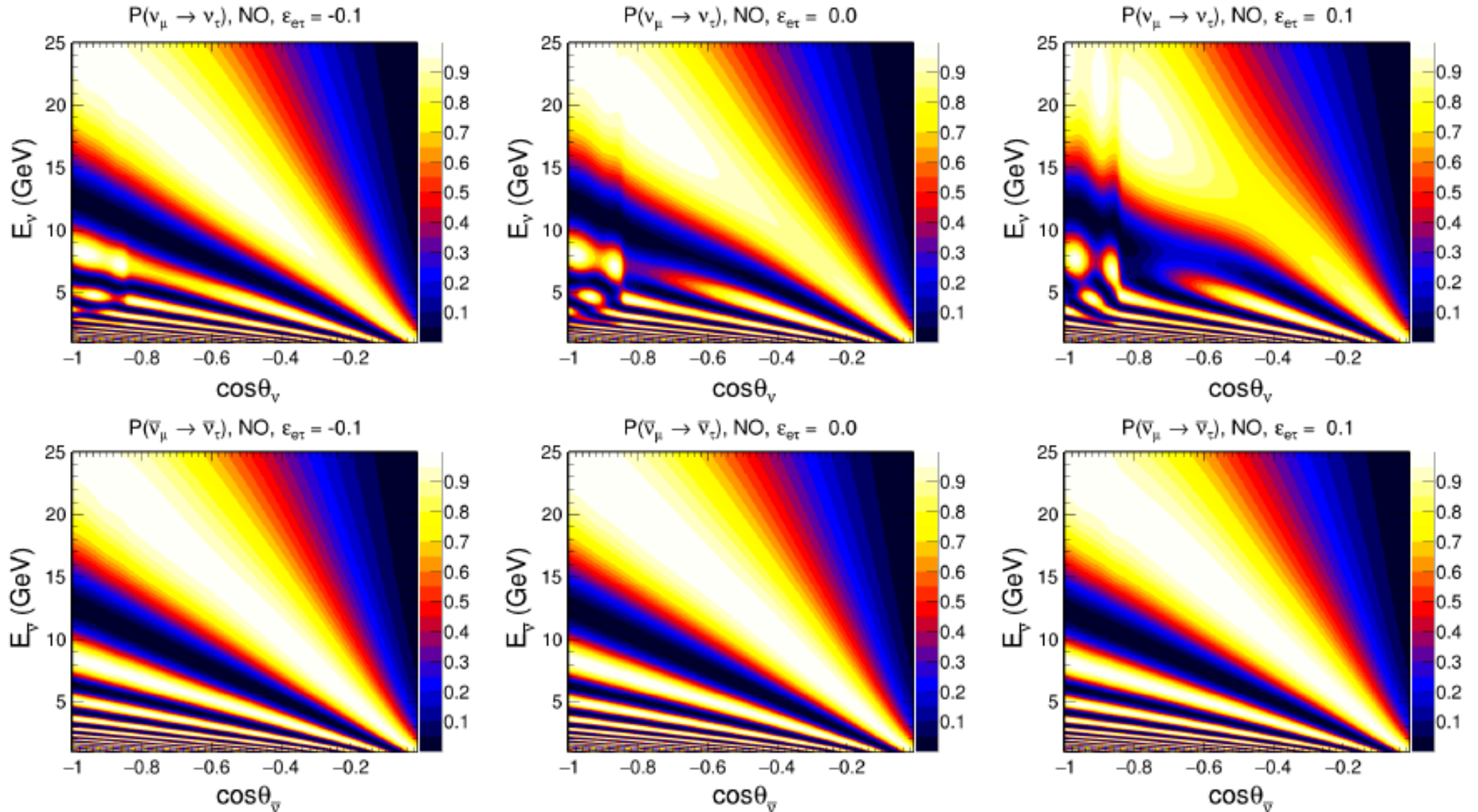


muon neutrino energy range: 1 GeV to 100 GeV  
muon neutrino zenith angle range ( $\cos\theta$ ): -1 to 1  
no detector properties are included

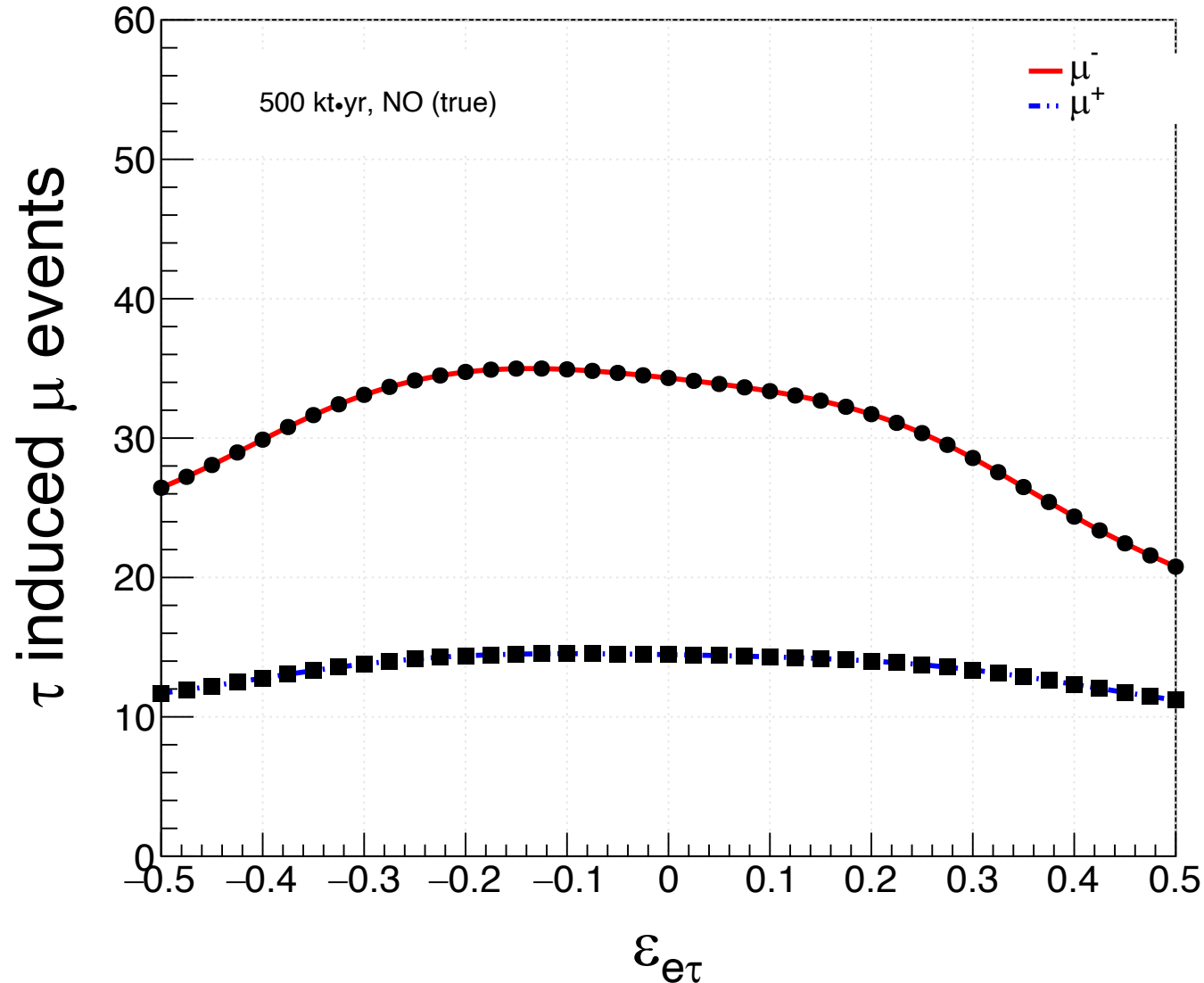
Kumar, Khatun, Agarwalla, in progress



# $\nu_\mu \rightarrow \nu_\tau$ transition with NSI parameter $\epsilon_{e\tau}$



# Muon events from Tau decay with NSI parameter $\epsilon_{e\tau}$



muon neutrino energy range: 1 GeV to 100 GeV  
muon neutrino zenith angle range ( $\cos\theta$ ): -1 to 1  
no detector properties are included

Kumar, Khatun, Agarwalla, in progress

# Concluding Remarks

Atmospheric neutrinos provide access to tau neutrinos and tau antineutrinos over a wide range of energies and baselines through mass-induced flavor oscillation

Since 2-3 mixing angle is close to maximal, the probability of  $\nu_{\mu} \rightarrow \nu_{\tau}$  transition is quite high around oscillation maxima

Detection of tau events will provide a direct access to oscillation maxima and oscillation valley

It can provide crucial information to test the deviation from maximal value of 2-3 mixing angle and to have a precise measurement of atmospheric oscillation parameters. It can also help in neutrino mass ordering measurements

It can also provide an unique window to probe beyond the Standard Model Physics like Non-Standard Interactions (NSIs), Lorentz Invariance Violation (LIV), Non-Unitary Neutrino Mixing (NUNM), Light eV-Scale Sterile Neutrino, and various others BSM scenarios

Statistics and systematics related to flux uncertainties are crucial bottlenecks

Need to have better reconstruction of hadron energies and directions in multi-GeV range

The overall prospects are quite high. So, lets keep working and exploring....

**Thank You**